Evaluation of NDVI for Monitoring Live Moisture in Three Vegetation Types of the Western U.S.

Colin C. Hardy and Robert E. Burgan

Abstract

The Normalized Difference Vegetation Index (NDVI) is evaluated for monitoring seasonal changes in live vegetation moisture. NDVI values for scenes of meadow grass, sagebrush, and an open-conifer stand were calculated using 0.5-m resolution multispectral images acquired from a fixed-wing aircraft four times from May to October, and live vegetation moisture was sampled simultaneously with each flight. Changes in sampled live vegetation moisture were compared with changes in the NDVI, and the proportion of seasonal change in NDVI attributable to changes in the understory vegetation rather than the conifer canopy was examined. Seasonal changes in vegetation moisture for all sites were statistically significant (p<0.05). Time-series profiles of the NDVI were functionally related to changes in vegetation moisture only for the grass and forest understory vegetation. No significant relationships were observed for either the shrub or coniferous forest canopy vegetation. This field experiment will improve our interpretation of seasonal NDVI data with respect to fire potential.

Introduction

The potential fire environment, or fire potential, for wildlands is assessed using information about fuels, weather, and topography. Information on the topography for a given site or area is generally well known — it doesn't change over time —and is increasingly available in the form of digitized elevation and terrain data. Knowledge of current weather and also of recent weather history is equally accessible for most fire-related applications. Wildland fuels include both living and dead biomass. It is necessary to know not only the amount of fuel (living and dead) but also the "condition" of each component of the fuel array. One of the principle attributes of vegetation condition required to assess its fire potential is fuel moisture. Models for fire behavior predictions and for fire danger rating depend on measured or estimated vegetation moisture inputs. The current moisture content of fine dead fuels (needles, leaves, cured herbaceous plants, and dead stems less than one-fourth inch in diameter) can be estimated from current weather observations and weather trends for several preceding days (Rothermel *et al.*, 1986). This ability is critical to same-day and next-day predictions of potential fire behavior. Forecasting of longer-term trends in fire potential, such as weekly or seasonal predictions, must also consider the condition of live vegetation. Historically, the moisture content of living vegetation has either

been estimated through empirically derived algorithms or was measured using intensive field methodology. Ideally, inexpensive, periodic, and repeatable assessments of the moisture of living and dead vegetation across large areas can provide fire planners and fuels managers valuable information.

An approach now being implemented in newly developed fire danger prediction systems is to exploit satellite technologies and products that can provide remotely sensed estimates of vegetation condition (Burgan and Bradshaw, 1996; Burgan *et al.*, 1997). The Advanced Very High Resolution Radiometer (AVHRR) sensor on board the TIROS-N series polar-orbiting weather satellites provides daily observations of the Earth's surface at a nominal spatial resolution (at nadir) of 1.1 square km. While it was not originally deployed with natural resource observation objectives, several indices derived from the AVHRR spectral data provide meaningful measures of vegetation condition (Loveland and Ohlen, 1993). The Normalized Difference Vegetation Index (NDVI), calculated from two bands of AVHRR data, is the difference in reflectance between the near-infrared and visible red wavelengths divided by the sum of the two measurements. As vegetation cures, its chlorophyll content is reduced and the visible (red) reflectance increases. At the same time, the near-infrared reflectance decreases. Therefore, NDVI is sensitive to the quantity of actively photosynthesizing biomass, and is useful for assessing changes in the fire environment resulting from seasonal vegetation phenology.

In their assessment of NDVI derived from the AVHRR sensor, Goward *et al.* (1991, p. 274) note "... given that the AVHRR sensor was not designed to study global vegetation patterns ... it is truly remarkable that this sensor provides at least monthly estimates of global vegetation dynamics with an error of approximately 10%." The difficulty in applying these data has become more evident in the recent shift from qualitative to quantitative interpretations. For example, if factors such as instrument precision and calibration, atmospheric interference, and off-nadir viewing are not accounted for, deviations between the satellite-derived indices and ground observations can easily exceed 50 percent (Goward *et al.*, 1991). Nonetheless, several studies have demonstrated potential applications of spectral data to assessments of vege-

USDA Forest Service, Rocky Mountain Research Station, P.O. Box 8089, Missoula, MT 59807 (chardy/rmrs_missoula@fs.fed.us).

tation condition, particularly in grasslands. In an extensive ground-sampling experiment at four locations in Australian grasslands, Paltridge and Barber (1988) established a relationship between fuel moisture content and a modified vegetation index from AVHRR data. They have developed an operational system for continuous monitoring of grassland fire danger potential using the AVHRR sensor. This system has been further improved through additional ground-truthing and verification of fuel moisture contents and also through the implementation of atmospheric corrective algorithms developed specifically for Australian grasslands (Paltridge and Mitchell, 1990).

While the Australian system is effective for grasslands, it's algorithms cannot be extrapolated to forested vegetation such as the coniferous forests widely common in the western United States. It is for just such coniferous forests that managers are most in need of indices that discriminate between the relatively moisture-stable conifer overstory and the surface grasses, shrubs, and herbaceous vegetation. Goward et al. (1985) and Nemani and Running (1989) found a strong relationship between measured surface temperatures (T_s) and NDVI (derived from AVHRR data), and they demonstrated that the slope of a T_s-NDVI curve could show changes in stomatal resistance to evapotranspiration by conifer forests. Reed et al. (1994) computed 12 phenologically linked metrics based on time-series NDVI and found strong coincidence between the satellite-derived metrics and predicted phenological characteristics. When these metrics were examined for several major land-cover types, they identified the interannual variability of spring wheat and the phenological fluxuations of shrublands, characterized the phenology of four types of grasslands, and verified the phenological consistency of deciduous and coniferous forests.

They conclude, however, by emphasizing that potential applications of satellite-derived metrics must be accompanied by detailed ground-truthing.

Detecting water stress from remotely sensed spectral data is difficult, particularly in coniferous canopies — a dominant lifeform with critical fire management implications in the western United States. Differences in responses can be caused by differences in species, morphology, understory rather than overstory signals, rock and bare soil interferences, and signal saturation. Riggs and Running (1991) analyzed differences in near-infrared reflectance features of water-stressed and control-forest canopies using a high-spectral-resolution imaging spectrometer. For the water-stressed treatment, the conifer stems were completely severed, then strapped upright to the stump. While differences in the spectral data were detected between the stressed and control treatments, Riggs and Running (1991) concluded that water stress in coniferous canopies could not be routinely detected at landscape scales by infrared reflectance alone. In two laboratory experiments, Cohen (1991) concluded that the use of vegetation indices (including NDVI) to predict water stress in leaves of lodgepole pine (*Pinus contorta*), Coulter pine (*Pinus coulteri*), ceanothus (*Ceanothus crassifolius*), and black sage (*Salvia mellifera*) appears limited.

Burgan and Hartford (1993) applied time-series NDVI when developing two greenness scales (relative and visual) for monitoring the timing and extent of seasonal changes in vegetation. While it is acknowledged that AVHRR-derived NDVI is responding to complex physiological changes in vegetation rather than simply to changes in moisture content alone, the relative greenness index provides a means by which actual live vegetation moisture *can* be estimated. Burgan et al. (1998) recently developed a Fire Potential Index (FPI) using maps of stylized fuel models, dead fuel moisture, and realtive greenness derived from AVHRR-NDVI (Burgan and Hartford, 1993) to determine the proportion of live and dead

vegetation. In their applications of FPI, Burgan et al. (1998) assume that both the quantity and moisture of live vegetation will be high when the relative greenness fraction approaches 1.0, where vegetation is as green as it can become. Conversely, both are assumed to be low when the relative greenness fraction is low. In field validations, they found the FPI to have a strong correlation with fire occurrence and was "... well adapted to portraying fire potential across both large geographic areas and for local areas down to a few square kilometers" (Burgan et al., 1998, pp. 159–170).

The evidence from these studies indicates that changes in NDVI response may be functionally related to, or at least coincident with, changes in the moisture condition of grasses, shrubs, and forest understory species. However, the relation of NDVI changes to the condition of coniferous overstory has not been well described. In their discussion of the various factors influencing the seasonal trends of NDVI of a forest canopy, Spanner et al. (1990a) emphasize the need to incorporate information about the mixed composition of an AVHRR pixel, where a mixture model could be used to determine the proportions of different reflecting surfaces. In a related study using relatively high spatial resolution (30-m) Thematic Mapper data, Spanner et al. (1990b) describe a family of spectral curves defining the relationship between Leaf Area Index (LAI) and the spectral response of coniferous canopies, and note that the appropriate curve is determined by the amount of understory vegetation as well as background reflectance contributing to the integrated signal received by the sensor. While it is an objective of some of these studies to filter out the effects of the understory vegetation on the overall spectral response of a target vegetation community, it is precisely the understory vegetation that is of most relevance to fire potential estimates. The understory vegetation comprises all of the fine fuels and surface fuels critical to both fire behavior and fire danger rating calculations.

A consistent difficulty in verifying relations between AVHRR data and vegetation condition or moisture is the relatively coarse spatial scale of the 1.1-km AVHRR data. Field personnel across the western United States collected samples intended to represent vegetation moisture across an entire 1-km² pixel (R. Bartlette, unpublished data on file). From this, it was learned that, for non-grassland situations, the high moisture variability within a 1-km² area made it infeasible to assess the relation of AVHRR-derived NDVI with vegetation moisture through paired-comparisons because of the difficulty of obtaining statistically valid vegetation moisture samples for varied vegetation over such a large area.

Objectives
This study is a time-series field experiment which assesses NDVI for monitoring vegetation moisture at a resolution appropriate for field verification, and has two primary objectives:

- Perform a time-series comparison of NDVI derived from high resolution multispectral images (acquired from aircraft) *with* concurrent field measurements of vegetation moisture content on three distinct vegetation types in the western U.S.; and
- Discriminate moisture and NDVI changes between coniferous forest canopy (overstory) and surface vegetation (understory) where the two vegetation strata occupy the same site — a structure common in coniferous forests of the western United States.

These two objectives required the acquisition of new spectral data at a spatial scale that allowed the spectral data to be compared with concurrent field measurements for at least four dates within the year of the study. It was not our intention to assess AVHRR-derived NDVI or to compare AVHRR data with this finer-resolution spectral data — there are currently

no suitable substitutes for AVHRR data in terms of either frequency or continental coverage. Rather, our focus was on the sub-AVHRR pixel behavior of vegetation moisture and NDVI.

Methodology

General Approach
The study design specified multi-date acquisition of vegetation moisture and spectral data for three distinct vegetation community types common to the northern Rocky Mountains: (1) grass-dominated, (2) shrub-dominated, and (3) an open-forest type where both moisture and spectral data could be discriminated between overstory coniferous canopy and understory vegetation. The three nearly flat study sites selected are located in western Montana. Each study area was surveyed and geo-located using a Global Positioning System (GPS) receiver and was nominally 5.4 hectares in area (200 meters wide by 270 meters long). Vegetation on the grass site was primarily wheatgrass (*Agropyron caninum*) and the shrub site was occupied almost exclusively by sagebrush (*Artemisia tridentata*). The shrub canopies occupied about 30 percent of the site. The overstory conifers in the open forest site were relatively evenly spaced (nominally 12 m apart) Douglas fir (*Pseudotsuga menziesii*) and ponderosa pine (*Pinus ponderosa*), about 35 years old. Ponderosa pine dominated the site, accounting for about 80 percent of the forest canopy. Total canopy coverage for the site was 40 percent. The understory species included sedge (*Carex geyeri*), Oregon grape (*Berberis repens*), snowberry (*Symphoricarpos albus*), pinegrass (*Calamagrostis rubescens*), and traces of other forbs.

Four sets of observations spanning the periods of greenup, flowering, curing, and senescence of the herbaceous and deciduous vegetation on each site were made in 1993. Vegetation sampling and image acquisition took place on 25 May, 15 July, 08 August, and, after full curing, on 09 October. Appropriate observation times were determined throughout the season by weekly visual observations of vegetation condition and also on the basis of cloud-free atmospheric conditions. The spectral data were acquired as close to solar noon as possible ($\pm$ 2 hours). An additional, fifth acquisition of spectral data took place on 29 January 1993, and was only done at the open forest study site. With snow on the ground (and not in the canopies), the winter data were acquired to create a trees-only mask to distinguish tree canopies from the understory vegetation.

Plot Area Registration Targets
Seven spatial control targets were permanently located at each study site for scene-to-scene (multi-date) image registration. One 2.4- by 2.4-m target was located at the plot area centroid (two flight-direction indicator panels complemented the center target). Additionally, we installed six 1.2- by 1.2-m targets within each site — one in each of the four corners and two located midway between the plot area centroid and diagonally opposing plot area corners. While as many as 15 control points are required for optimum registration, these seven spatial control targets provided consistent, visible, fixed points from which to initiate the multi-scene registration process. Other natural features identified within each of the sites complete the suite of pre-established control points used for registration.

Spectral Image Acquisition
We acquired 0.5-m^2 spatial-resolution scenes of each site with a multispectral imaging system deployed on a fixed-wing aircraft. The first generation (1992) Airborne Data Acquisition and Registration (ADAR) 5000 System, developed and operated by Positive Systems, Inc. of Whitefish, Mon-

TABLE 1. SPECTRAL CHARACTERISTICS OF THE ADAR5000 AND AVHRR BANDS USED IN THE STUDY

Spectral Band	Sensor Band	Nominal Range
		Nanometers
Red	AVHRR$_1$	580–680
	ADAR$_2$	597–677
NIR	AVHRR$_2$	725–1100
	ADAR$_4$	800–1000

tana, uses four charged-coupled-device (CCD) sensors, each configured with a filter to obtain a unique spectral wavelength[1]. Each CCD sensor had 359,154 pixels (739 by 486), with a 22-degree field of view in the major axis direction. The spectral characteristics for the ADAR 5000 configuration used in this study to mimic AVHRR bandpasses are presented in Table 1.

The sensors and a GPS receiver are controlled by an onboard RISC-based workstation, which performs analog-to-digital conversions, stores the digital data, and provides on-screen, near-real-time statistics and verifies scene acquisition. Navigational way points established using GPS coordinates obtained on each site were used to control the aircraft flight orientation and elevation. Spatial resolution in the image data of 0.5-m square per pixel was obtained for each site by flying the aircraft at a predetermined elevation of 915 meters above ground level. While the ADAR 5000 allows sensor gain (aperture) to be adjusted to optimize image statistics, a predetermined aperture was used for all observations to control for changes in image density. We did not correct the data for atmospheric interference, because the surface-to-sensor distance was less than one-thousand meters and because of the relatively aerosol-free atmosphere in the area of the study.

Calculating NDVI with ADAR 5000 Data
The spectral distribution of the four sensors on the ADAR 5000 differs somewhat from that of the AVHRR sensor. However, Band 2 of ADAR 5000 data most closely resembles the wavelength/bandwidth of AVHRR visible red (channel 1), and Band 4 of ADAR 5000 is nearly identical to the near-infrared channel (channel 2) of AVHRR (Table 1). We were thereby able to substitute ADAR 5000 Bands 2 and 4 directly for AVHRR channels 1 and 2, respectively, to calculate NDVI. The $NDVI_{Raw}$ calculated in Equation 1 is not corrected for solar angle: i.e.,

$$NDVI_{Raw} = \frac{(b_4 - b_2)}{(b_4 + b_2)} \qquad (1)$$

where b_2 = ADAR5000 Band 2 and b_4 = ADAR5000 Band 4.

Vegetation Moisture Sampling
Vegetation sampling was done simultaneously with the spectral data flights ($\pm$ 2 hours), and was manually clipped from 12 plots within each of the grass and shrub study sites and also for the understory vegetation on the open-forest site. For each observation time, three parallel sampling transects were established along the long axis of each study site. Four vegetation sampling plots were then evenly distributed along each of the three transects. Because of the destructive nature of the sampling, the precise locations for clipping were changed for each observation date by randomly locating the sampling plots along the three traverses within each study site. Vegetation was then clipped from within a 1-m^2 area at

---

[1] The use of trade or firm names in this publication is for reader information and does not imply endorsement by the U.S. Department of Agriculture of any product or service.

| TABLE 2. | DISTRIBUTION OF PIXELS REPRESENTING TREES-ONLY, UNDERSTORY, RIND, AND ZERO DATA FOR THE OPEN-FOREST SITE |

Pixel Category	Distribution of Pixels by Date			
	05/25	07/15	08/12	10/09
	Number of pixels (%)			
Trees Only	12361 (12)	12302 (12)	11752 (12)	12167 (12)
Understory	62683 (62)	62940 (63)	62636 (62)	60043 (60)
Rind	15350 (15)	15350 (15)	15350 (15)	15350 (15)
Zero Data	10211 (10)	10013 (10)	10867 (11)	13045 (13)
Total	100605	100605	100605	100605

TABLE 3. MEAN NDVI AND MOISTURE CONTENT (H_2O) FOR EACH VEGETATION CATEGORY, BY OBSERVATION DATE

	Forest Site				Grass Site		Shrub Site	
	Trees Only		Understory					
Date	NDVI	H_2O	NDVI	H_2O	NDVI	H_2O	NDVI	H_2O
25 May	0.53	87%	0.42	256%	0.33	170%	0.16	144%
15 Jul	0.52	113%	0.40	148%	0.23	147%	0.14	152%
12 Aug	0.45	116%	0.34	107%	0.09	54%	0.09	119%
09 Oct	0.60	112%	0.38	72%	0.14	26%	0.15	72%

category remained constant at 12 percent, the proportion of pixels in the understory category decreased somewhat — from 63 percent in July to 60 percent by the October date — due to the elimination of a greater number of deeply shadowed pixels. The spatial distribution of these categories is illustrated in Plate 1, where panel 1a shows the original false-color composite (RGB) of the open-forest site, and panel 1b illustrates trees, rind, and understory, which are shown as black, white, and gray, respectively.

NDVI for the Open-Forest Site
The NDVI for the understory category of the open-forest site ranged from 0.34 to 0.42 (Table 3). The absolute change, or percent deflection from the maximum value, was roughly 19 percent. In contrast, the NDVI values for the trees were higher, ranging from 0.45 to 0.60 (Table 3), with a corresponding absolute change of 12 percent. The NDVI seasonal profile for the total open-forest scene can be compared with the trees-only and understory profiles in Figure 1. The overall NDVI for the open-forest site is heavily weighted towards the understory, because over 60 percent of the pixels used in the NDVI calculation for the open-forest site represent understory vegetation. However, the seasonal profile for the total open-forest scene is similar to other time-series profiles of NDVI for coniferous forests. For example, both the general shape of the NDVI profiles and the absolute values for our data are similar to seasonal NDVI profiles derived from The-
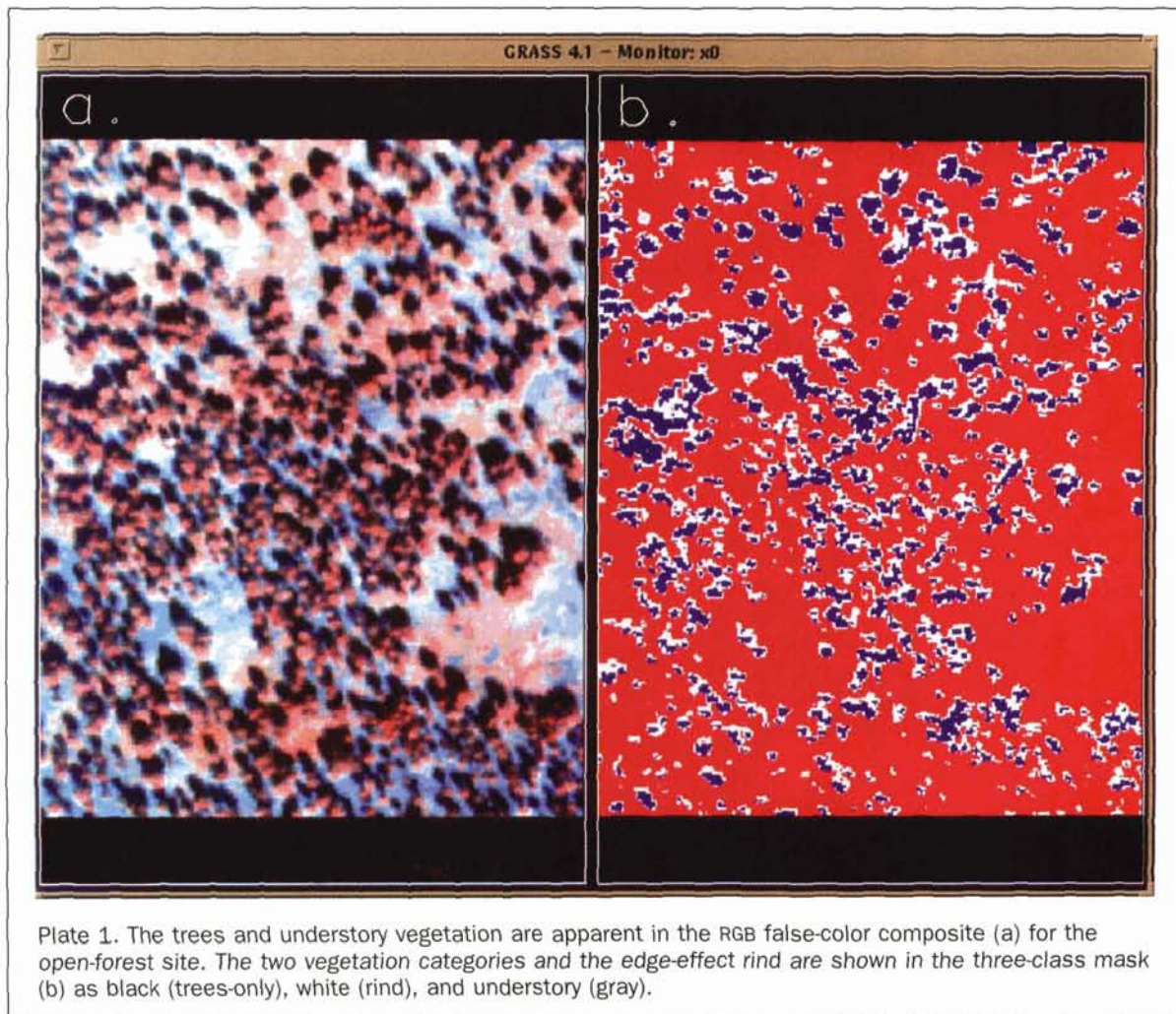

Plate 1. The trees and understory vegetation are apparent in the RGB false-color composite (a) for the open-forest site. The two vegetation categories and the edge-effect rind are shown in the three-class mask (b) as black (trees-only), white (rind), and understory (gray).

each plot location. Three overstory samples were obtained from each of 12 permanently located sample trees in the open forest site by shooting foliated branch ends from three sides of each tree with a shotgun. The mean moisture content of the vegetation at each site was then determined gravimetrically. The individual vegetation samples were stored in air-tight containers and weighed before and after oven-drying at 100°C for 36 hours. The pre- and post-drying mass values were used to calculate the percentage moisture content for each sample. The simple average of all samples for a site represents the mean moisture content.

Image Analysis

Band-to-Band Rectification
Although we ultimately used only two of four ADAR 5000 spectral bands (Band 2 [red] and Band 4 [NIR]), we retained all four bands throughout the analysis. The four bands from each ADAR5000 scene were band-to-band rectified by the vendor prior to our analysis, essentially creating a four-band image suitable for conventional image analysis software.[2]

Registration
The spectral data acquired on the four observation dates for a given study site were registered to the 25 May scene because that date was the first. Because the imaged areas for the four dates were not identical, we defined an initial region for each study site large enough to contain all four scenes prior to registration. We then created two additional image layers: the NDVI using Equation 1, and a false-color composite (RGB) for visual reference only. The RGB image provided the best visual interpretation and enabled the identification of registration control points. The image registration functions we used registered all six image layers (b1, b2, b3, b4, NDVI, RGB) simultaneously. The overall root-mean-square (RMS) registration errors for all dates of the open-forest and shrub scenes ranged between 0.78 and 0.91 pixels. The grass scenes were not registered because the general homogeneity of the vegetation made it unnecessary. Following registration, pixel counts were identical and relative locations of pixels were assumed to be the same (within the stated RMS errors) for all data from a given study area.

Eliminating Shadow Effects
Through interactive subjective inspection of the RGB data, we found that areas within the scenes shadowed by overstory trees had RGB values of zero. Some of these zero-data pixels were artifacts of our specification that sensor apertures remain constant for all dates, thereby resulting in under-exposure within dark shadow areas. Any pixel in the NDVI data whose corresponding RGB value was zero was also set to zero.

Discriminating between Forest Canopy and Understory for the Open-Forest Study Site
While the moisture samples from forest canopy foliage (trees) and the understory foliage (understory) were treated separately, further image analysis procedures were required to discriminate changes in NDVI values between the overstory and the understory. Because the registration errors indicated that a pixel's location from one scene to another could be off by as much as 0.91 pixels, our approach for discriminating between trees and understory was conservative to eliminate any "edge effects."

---

[2] We used the image analysis functions in GRASS 4.1, developed by U.S. Army Corps of Engineers Construction Engineering Research Laboratories.

To create a mutually exclusive tree-versus-understory mask, we acquired a spectral scene in the winter when the understory vegetation was snow-covered but the tree canopies were clearly snow-free (the thinner snow layer in the tree canopies had melted through solar exposure). Manual interrogation of the winter NDVI data associated with pixels that were clearly tree crowns indicated they had NDVI values of 0.31 or greater. Pixels representing understory vegetation had NDVI values of 0.18 or less because they were covered with snow. Those pixels having NDVI values ranging between 0.19 to 0.30 were considered to represent edges of tree crowns, or were within the 0.91-RMS rectification error where grid-cell overlap could occur between observation dates. These edge-effect pixels, termed "rind," were excluded from the analysis. With this information we created separate zero/one masks that identified pure tree crown or pure understory pixels.

Calculating the Mean NDVI for Each Scene
Frequency distributions of pixel count by NDVI value were calculated for each observation date. The shrub and grass sites required no masking of shadow or overstory. For the open-forest study site, the zero/one tree and understory masks were used to obtain NDVI frequency distributions representing each respective vegetation component (trees and understory). Additional frequency distributions were derived for the overall open-forest using the entire unmasked scenes. The frequency distributions were then used to calculate a mean NDVI for each scene.

Correcting the Mean NDVI Values for Changes in Solar Zenith
Changes in the solar zenith angle significantly effects NDVI. A decrement of as high as 33 percent of maximum can occur when the solar zenith angle reaches 70 degrees (Singh, 1988). In the case of the present study, controlling for changes in solar angle was critical because of our interest in the temporal aspects of the data, whose acquisition dates span nearly a six-month period. Two general approaches have been employed with NDVI data to account for solar zenith angle. The first approach is to correct the raw radiance values prior to calculation of NDVI. Spanner *et al.* (1990) have done this using an equation from Smith *et al.* (1980). The second approach — a direct first-order correction — is to correct the NDVI values directly. This approach, presented in Singh (1988), has been used by Curran *et al.* (1992) in a time-series study similar to the present study. Corrections are not appropriate for solar zenith angles less than 30 degrees or greater than 70 degrees (Singh, 1988). The net NDVI correction for solar zenith angles smaller than 30 degrees is less than one percent. Only two of our four seasonal observations were acquired under solar zenith angles greater than 30 degrees — 31.9 degrees for 08 August and 53.5 degrees for 09 October. We corrected the $NDVI_{raw}$ values for the August and October scenes using the procedures detailed by Singh (1988) to obtain the final NDVI presented in the results. While the corrections changed the August NDVI values by less than 1 percent, the October NDVI values reported below are approximately 22 percent higher than the uncorrected $NDVI_{raw}$.

Results and Discussion

Trees versus Understory on the Open-Forest Site
Two unique, mutually exclusive data sets were discriminated from the open-forest NDVI spectral data: trees-only and understory. A third data set, called "rind," represents pixels excluded entirely from the analysis. The distribution of these data for the four observation dates is given in Table 2. While the proportion of the total data allocated to the trees-only
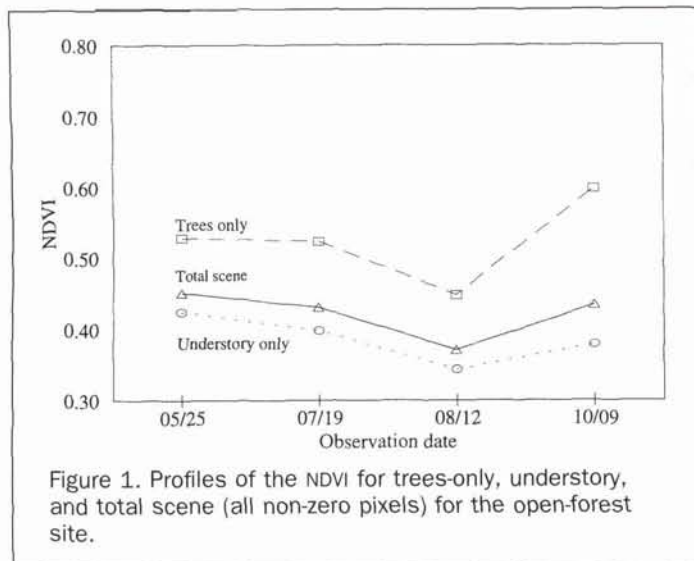
Figure 1. Profiles of the NDVI for trees-only, understory, and total scene (all non-zero pixels) for the open-forest site.

matic Mapper Simulator (TMS) observations made by Spanner *et al.* (1994) over a transect of young ponderosa pine in western Oregon.

Measured Vegetation Moisture

The mean vegetation moisture contents (percent of ovendry weight) from all of the observations are given in Table 3, and the data are also plotted with their 95 percent confidence intervals ($p<0.05$) in Figure 2. For the trees-only data, the only significant difference in moisture content is between the first observation (05/25) and the other three dates ($p<0.05$). This agrees with numerous other observations of the moisture-regulating efficiency of coniferous forest species (Riggs and Running, 1991). However, the moisture content of the understory decreases significantly at each of the three successive time steps (p-values for the June, August, and October time steps were 0.0041, 0.0086, and 0.0269, respectively. At the grass site, each successive observation of moisture content was significantly lower than its preceding value ($p<0.05$). Moisture content observed at the shrub site decreased significantly at all but the first time step.

NDVI Relations with Moisture Content

The relations between NDVI and moisture content for the four vegetation categories are shown in Figure 2. While ratios such as NDVI can be shown to be related to vegetation condition, Spanner *et al.* (1990) note that the strength of the relationships in coniferous forest sites is affected by many site and vegetation-related variables such as canopy closure, understory vegetation, and background contributions to the spectral radiance. While having only four time-series observations restricts our ability to draw strong conclusions regarding the data, we performed simple linear regression analyses to illustrate the functional relationships between NDVI and moisture content for the grass and understory data. Statistical results for the regressions are shown in Table 4, where the coefficient of determination (R^2) is highest for the grass data. The relationship was not as strong for the under-

story data. The functional relationships for both the grass data and understory data are plotted in Figure 3. Because the moisture and NDVI data are considerably different between the two vegetation categories, the regression equations are quite different in both slope and y-intercept. Because grasses covered 100 percent of the grass site with no visible exposed soil, all of the change in NDVI can be attributed to changes in the condition of the grass.

Within the forest site, only the understory vegetation is related to changes in NDVI. Because the understory comprised only 60 percent of the pixels, large changes in understory moisture are associated with relatively small changes in NDVI. A single regression equation derived from the combination of grass and understory data was clearly not appropriate. Further, the linear regression equations (Table 4) and their associated plots shown in Figure 3 are not intended to imply causality. Numerous physiological and phenological changes in the vegetation and on the site contribute to changes in the radiance values from which NDVI is calculated. Changes in vegetation moisture alone typically accompany, rather than directly cause, these physical changes.

Conclusions

The purpose of this study was to assess the relations between changes in very high resolution NDVI and changes in vegetation moisture content on three distinct vegetation types in the western United States. This field experiment was an attempt to discriminate changes in moisture and NDVI changes between coniferous forest canopy (overstory) and surface vegetation (understory) where the two vegetation strata occupied the same site — a structure common in coniferous forests of the western United States. A better understanding of these relationships will contribute to the use of remotely sensed spectral data in the development of an index (or indices) to represent current or seasonal trends in fire potential.

Significant seasonal changes in vegetation moisture were measured for grass, shrub, and open-forest understory vegetation. The greatest observed change in vegetation moisture was in the open-forest understory vegetation. After initial spring flushing, the moisture content of the coniferous forest canopy foliage evaluated in this study was relatively stable, with no significant changes from July through October.

The spectral data acquired during the winter when the ground was fully masked by snow (and the overstory trees were snow-free) provided an optimal scene to utilize when discriminating pixels of overstory trees versus the understory vegetation. This facilitated derivation of separate seasonal NDVI themes for each of four vegetation types, including separate profiles for the coniferous canopy and understory within the open-forest study site.

No meaningful relationship between changes in vegetation moisture and seasonal NDVI profiles was detected for either the shrub site or the trees-only data. While only two degrees of freedom limits the statistical significance of the relationships between changes in NDVI and moisture content, we have presented the functional relationships between NDVI and moisture content for both the grass site and open-forest understory, which share similar physical characteristics. These results support the general evidence reported in other work in grass and related vegetation. Data from the open-forest site, where over 60 percent of the pixels in the spectral data represented understory vegetation, clearly reinforce the need to account for mixed vegetation composition when inferring vegetation condition from spectral data.

This sub-AVHRR pixel field experiment suggests that AVHRR-scale NDVI appears to have limited applicability for monitoring seasonal changes in actual vegetation moisture content of brush sites such as the one in this study, which had relatively low canopy closure. However, this sub-pixel,

TABLE 4. STATISTICAL SUMMARY FROM SIMPLE REGRESSION ANALYSES

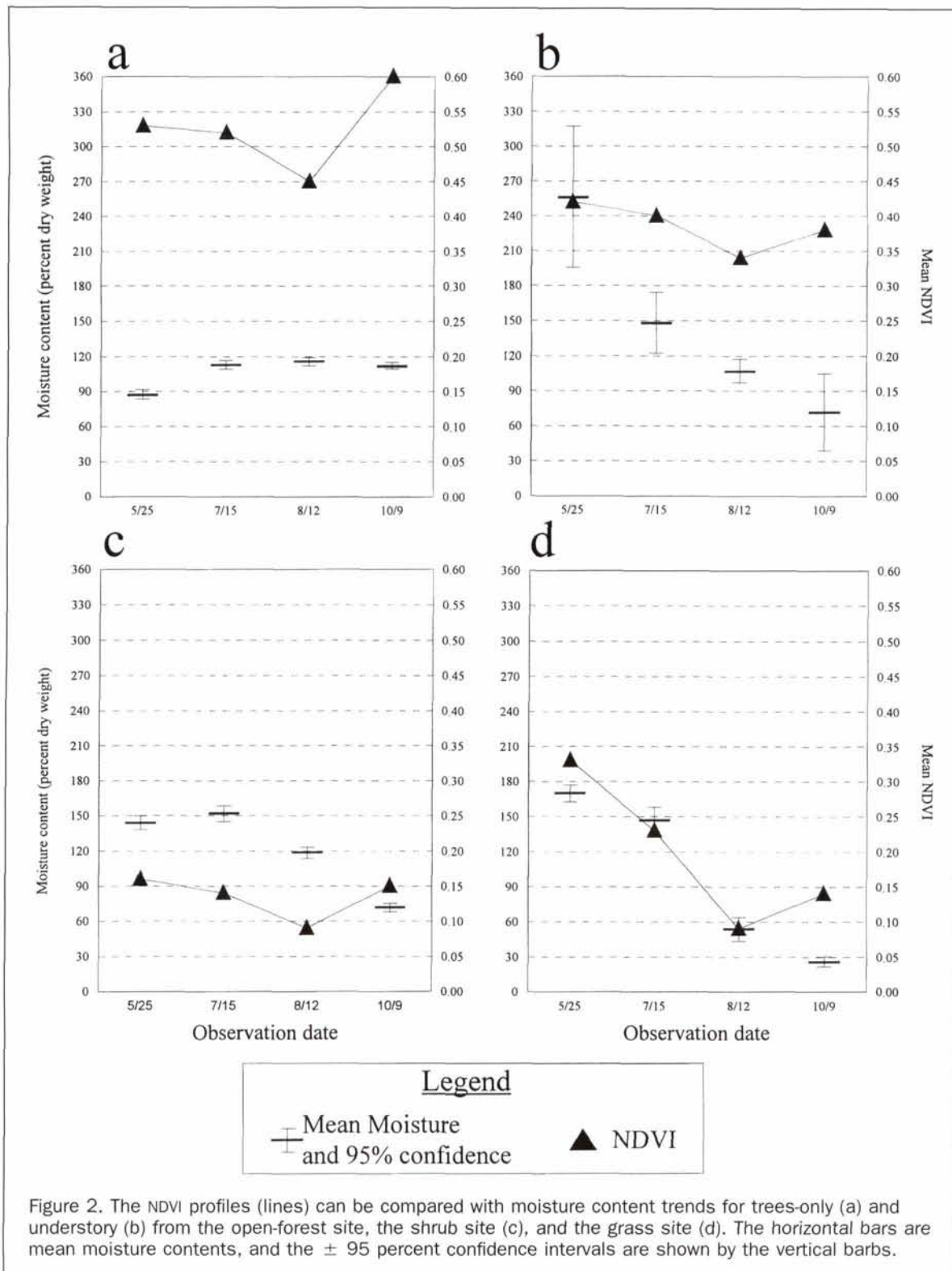| Datum	Degrees of Freedom	R^2	Constant	X-coeff.	Std. error of Y-est.
Grass	2	.815	−0.1872	5.964	0.367
Understory	2	.539	−5.1465	17.162	0.664

Figure 2. The NDVI profiles (lines) can be compared with moisture content trends for trees-only (a) and understory (b) from the open-forest site, the shrub site (c), and the grass site (d). The horizontal bars are mean moisture contents, and the ± 95 percent confidence intervals are shown by the vertical barbs.

mixed vegetation composition is clearly less of a constraint to the use of AVHRR-scale NDVI data in non-forested areas of the western United States, where the data appear useful for monitoring changes in the moisture content of grasslands, and also of vegetation beneath forests having less than about 50 percent crown closure. It is these two vegetation community types for which fire potential indices are quite critical, however, and this study has enhanced our understanding

of sub-AVHRR pixel behavior and, more importantly, has improved our ability to interpret AVHRR-NDVI towards the development of the Fire Potential Index.

The limited sample size was a recognized statistical constraint in our experimental design. Additionally, we recognize that the NDVI ratio does not utilize the spectral band most sensitive to moisture (1.7 to 2.9 micrometers). Therefore, we did not verify statistical correlation or causal rela-
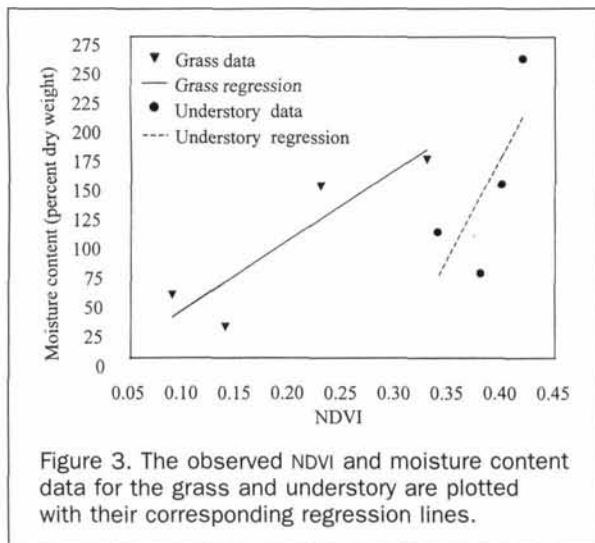
Figure 3. The observed NDVI and moisture content data for the grass and understory are plotted with their corresponding regression lines.

tionships. Rather, we have demonstrated strong coincidence in the functional relationships between changes in NDVI and vegetation moisture. These results are corroborated by numerous theoretical studies relating to vegetation phenology and the spectral characteristics of various sensors and reflecting surfaces.

References

Burgan, R.E., and R.A. Hartford, 1993. *Monitoring Vegetation Greenness with Satellite Data*, USDA For. Serv. Gen. Tech. Rep. INT-297, 13 p.

Burgan, R.E., and L.S. Bradshaw, 1996. Weather needs for the wildland fire assessment system, *Proceedings of the 22nd Conference on Agricultural and Forest Meteorology with Symposium on Fire and Forest Meteorology*, 28 January to 02 February, Atlanta, Georgia, American Meteorological Association, Boston, Massachusetts, pp. 325–328.

Burgan, R.E., P.L. Andrews, L.S. Bradshaw, C.H. Chase, R.A. Hartford, and D.J. Latham, 1997. Current status of the Wildland Fire Assessment System (WFAS), *Fire Management Notes*, 57(2):14–17.

Burgan, R.E., R.W. Klaver, and J.M. Klaver, 1998. Fuel models and fire potential from satellite and surface observations, *International Journal of Wildland Fire* 8(3):159–170.

Cohen, W.B., 1991. Response of vegetation indices to changes in three measures of leaf water stress, *Photogrammetric Engineering & Remote Sensing*, 57(2):195–202.

Curran, P.J., J.L. Dungan, and H.L Gholz, 1992. Seasonal LAI in slash pine estimated with Landsat TM, *Remote Sensing of Environment*, 39:3–13.

Goward, S.N., G.D. Cruickshank, and A.S. Hope, 1985. Observed relations between thermal emission and reflected spectral radiance of a complex vegetated landscape, *Remote Sensing of Environment*, 18:137–146.

Goward, S.N., B. Markham, D.G. Dye, W. Dulaney, and J. Yang, 1991. Normalized difference vegetation index measurements from the advanced very high resolution radiometer, *Remote Sensing of Environment*, 35:257–271.

Loveland, T.R., and D.O. Ohlen, 1993. Experimental AVHRR land data sets for environmental monitoring and modeling, *Environmental Modeling with GIS* (M.F. Goodchild, B.O. Parks, and L.T. Steyaert, editors), Oxford University Press, New York, pp. 379–385.

Nemani, R.R., and S.W. Running, 1989. Estimation of regional surface resistance to evapotranspiration from NDVI and thermal-IR AVHRR data, *J. of Appl. Meteorol.*, 28:276–284.

Paltridge, G.W., and J. Barber, 1988. Monitoring grassland dryness and fire potential in Australia with NOAA/AVHRR data, *Remote Sensing of Environment*, 25:381–394.

Paltridge, G.W., and R.M. Mitchell, 1990. Atmospheric and viewing angle correction of vegetation indices and grassland fuel moisture content derived from NOAA/AVHRR, *Remote Sensing of Environment*, 31:121–135.

Riggs, G.A., and S.W. Running, 1991. Detection of canopy water stress in conifers using the airborne imaging spectrometer, *Remote Sensing of Environment*, 35:51–68.

Singh, S.M., 1988. Simulation of solar zenith angle effect on global vegetation index (GVI) data, *International Journal of Remote Sensing*, 9(2):237–248.

Spanner, M.A., L.L Pierce, S.W. Running, and D.L. Peterson, 1990a. The seasonality of AVHRR data of temperate coniferous forests: relationship with leaf area index, *Remote Sensing of Environment*, 33:97–112.

————, 1990b. The seasonality of AVHRR data of temperate coniferous forests: relationship with leaf area index, *Remote Sensing of Environment*, 33:97–112.

Spanner, M.A., L. Johnson, J. Miller, R. McCreight, J. Freemantle, J. Runyun, and P. Gong, 1994. Remote sensing of seasonal leaf area index across the Oregon transect, *Ecological Applications*, 4(2):258–271.